



NLR-TP-99408

Corrosion and fatigue assessment of aircraft pressure cabin longitudinal lap splices

R.J.H. Wanhill

Nationaal Lucht- en Ruimtevaartlaboratorium

National Aerospace Laboratory NLR

Anthony Fokkerweg 2

P.O. Box 90502

1006 BM Amsterdam

The Netherlands

Telephone +31 (0)88 511 31 13

Fax +31 (0)88 511 32 10

www.nlr.nl

DOCUMENT CONTROL SHEET

	ORIGINATOR'S REF. NLR-TP-99408		SECURITY CLASS. Unclassified										
ORIGINATOR National Aerospace Laboratory NLR, Amsterdam, The Netherlands													
TITLE Corrosion and fatigue assessment of aircraft pressure cabin longitudinal lap splices													
PUBLISHED IN: The proceedings of the 5th International Aerospace Corrosion Control Symposium, 3-5 November, 1999, Amsterdam													
AUTHORS R.J.H. Wanhill		DATE 22 September 1999	<table style="width: 100%; border-collapse: collapse;"> <tr> <td style="width: 50%;">pp</td> <td style="width: 50%;">ref</td> </tr> <tr> <td style="text-align: center;">42</td> <td style="text-align: center;">26</td> </tr> </table>	pp	ref	42	26						
pp	ref												
42	26												
DESCRIPTORS <table style="width: 100%; border-collapse: collapse;"> <tr> <td style="width: 50%;">Aircraft structures</td> <td style="width: 50%;">Fatigue life</td> </tr> <tr> <td>Corrosion</td> <td>Fuselages</td> </tr> <tr> <td>Crack initiation</td> <td>Pressurized cabins</td> </tr> <tr> <td>Crack propagation</td> <td>Transport aircraft</td> </tr> <tr> <td>Fatigue (materials)</td> <td></td> </tr> </table>				Aircraft structures	Fatigue life	Corrosion	Fuselages	Crack initiation	Pressurized cabins	Crack propagation	Transport aircraft	Fatigue (materials)	
Aircraft structures	Fatigue life												
Corrosion	Fuselages												
Crack initiation	Pressurized cabins												
Crack propagation	Transport aircraft												
Fatigue (materials)													
ABSTRACT Because aircraft structures are susceptible to corrosion and fatigue damage, which concentrate at joints, there is a possibility of interactions between corrosion and fatigue, especially as aircraft become older. Of particular concern are the longitudinal lap splices of transport aircraft pressure cabins. This paper reports on the disassembly and investigation of lap splices from several types of transport aircraft. Broadly speaking, the investigation showed that pressure cabin longitudinal lap splices have a corrosion problem or a fatigue problem: severe corrosion does not result in Multiple Site Damage (MSD) fatigue cracking, and MSD is not initiated by corrosion. However, there is evidence of a mild environmental effect on MSD fatigue crack growth. The results are discussed with respect to MSD fatigue modelling and simulation and lap splice fatigue analysis methods.													



NLR-TP-99408

Corrosion and fatigue assessment of aircraft pressure cabin longitudinal lap splices

R.J.H. Wanhill

This paper has been prepared for publication in the proceedings of the 5th International Aerospace Corrosion Control Symposium, 3-5 November, 1999, Amsterdam.

The contents of this report may be cited on condition that full credit is given to NLR and the author(s).

Division: Structures and Materials
Issued: September 1999
Classification of title: Unclassified



Contents

INTRODUCTION	5
LAP SLICE POSITIONS AND CONFIGURATIONS	6
CORROSION	6
FATIGUE	9
MSD FATIGUE MODELLING AND SIMULATION	14
DISCUSSION	17
CONCLUSIONS	19
REFERENCES	20

5 Tables
23 Figures

(42 pages in total)



This page is intentionally left blank.



CORROSION AND FATIGUE ASSESSMENT OF AIRCRAFT PRESSURE CABIN LONGITUDINAL LAP SPLICES

R.J.H. Wanhill, National Aerospace Laboratory NLR, Amsterdam

Because aircraft structures are susceptible to corrosion and fatigue damage, which concentrate at joints, there is a possibility of interactions between corrosion and fatigue, especially as aircraft become older. Of particular concern are the longitudinal lap splices of transport aircraft pressure cabins. This paper reports on the disassembly and investigation of lap splices from several types of transport aircraft. Broadly speaking, the investigation showed that pressure cabin longitudinal lap splices have a corrosion problem or a fatigue problem: severe corrosion does not result in Multiple Site Damage (MSD) fatigue cracking, and MSD is not initiated by corrosion. However, there is evidence of a mild environmental effect on MSD fatigue crack growth. The results are discussed with respect to MSD fatigue modelling and simulation and lap splice fatigue analysis methods.

INTRODUCTION

Aircraft are susceptible to corrosion and fatigue damage, which concentrate at structural joints. There is a possibility – often assumed to be a certainty – of interactions between corrosion and fatigue, especially as aircraft age. Of particular concern are the longitudinal lap splices of transport aircraft pressure cabins. The Aloha Airlines incident (1) showed that corrosion (disbonding of a lap splice and associated fail-safe tear straps) in combination with Multiple Site fatigue Damage (MSD) along the lap splice can lead to a sudden and potentially catastrophic loss of structural integrity.

However, although corrosion contributed to the Aloha Airlines incident, it was not directly implicated in the initiation of fatigue cracks: rather, it was the lap splice debonding that enabled stress concentrations at the rivet holes and mechanically-induced MSD (1).

This paper reports on the disassembly and investigation of longitudinal lap splices from several types of transport aircraft with a view to determining

- (1) The characteristics of corrosion and MSD fatigue crack initiation and early crack growth.
- (2) Any associations between corrosion and MSD.



(3) Suitable MSD fatigue modelling and simulation, and lap splice fatigue analysis methods.

The lap splices came from five service aircraft, a Boeing B 727-100, three Fokker F28s and a British Aerospace BAC 1-11, and the Fokker F100 full-scale fuselage test. The histories of all six pressure cabins are summarised in table 1.

Table 1 Service or test histories of the pressure cabins

Aircraft type	Flights	Flight hours	Simulated flights
B 727-100	53,424	59,848	126,250 @ 110 % design load
F28-1000	34,470	unknown	
F28-4000 [1]	43,870	28,694	
[2]	43,323	unknown	
F100			
BAC 1-11	75,158	52,000	

LAP SPLICE POSITIONS AND CONFIGURATIONS

Figures 1-3 show the positions and configurations of the lap splice samples. The positions varied widely, as do the joint designs. The single common feature is the sheet material, 2024-T3 Alclad.

CORROSION

B 727-100 service aircraft

The B 727-100 lap splice sample was provided by the Institute for Aerospace Research (IAR) in Ottawa, Canada. The sample was one of several taken from aircraft inspected with the D Sight Aircraft Inspection System (DAIS) (2). Figure 4 gives an external overview of the sample and a detail of the *internally* visible corrosion. The corrosion appeared to be concentrated along the upper side of the lap splice/stiffener connection, but the DAIS showed that corrosion-induced “pillowing” was present throughout the lap splice, figure 5.

After sample removal the IAR carried out eddy current and X-ray radiography non-destructive inspection (3) before sending it to the NLR. The sample was then again inspected using eddy current (4). Figure 6 shows the results of non-destructive inspection, which was to determine the



severely corroded area and any cracking associated with rivet locations along the lap splice. The severe corrosion was found to be in a well-defined area covering all three rivet rows of the lap splice. However, the crack indications were almost all confined to the upper rivet row: only two indications were outside the severely corroded area.

The lap splice sample was then disassembled and examined by the NLR for cracks. The procedure is given in table 2.

Table 2 B 727-100 lap splice sample disassembly and examination for cracks

<ul style="list-style-type: none">• Macroscopic/mesoscopic<ul style="list-style-type: none">• removal of sub-samples containing the rivet rows• sectioning rivet holes, removal of rivets and lap splice disassembly (4)• visual screening (50 × binocular) for cracks in lap splice sheets and stringer base• Mesoscopic/microscopic<ul style="list-style-type: none">• opening-up sectioned rivet holes suspected or already found to be cracked (4)• visual screening (50 × binocular) for fracture surface appearances• Scanning Electron Microscopy (SEM) for fracture identification

Figures 7 and 8 show the types and locations of cracks found in the outer and inner sheets of the lap splice (no cracks were found in the stringer base) and figure 9 compares the results of disassembly with those of non-destructive inspection. There are four main points to note:

- (1) Almost 95 % of the cracking, in terms of crack locations, was intergranular owing to exfoliation corrosion and stress corrosion, the latter especially as corrosion products built up between the sheets to cause locally high stresses (5). Some of the larger intergranular cracks were associated with small, secondary fatigue cracks. These usually initiated from intergranular cracking, but sometimes occurred directly from rivet holes, without any evidence of fatigue initiation due to local corrosion (pitting). Figure 10 shows examples of these associations.
- (2) The rivet hole locations determined to be only fatigue cracked showed no evidence of fatigue initiation due to local corrosion (pitting). These cracks will be discussed further in the FATIGUE section of this paper.



- (3) Only the severest cracking, along the upper rivet row (with one exception), was detected by X-ray radiography and eddy current non-destructive inspections.
- (4) Comparison of figure 5 with figures 7-9 seems to indicate that the DAIS is more sensitive to detecting severe corrosion than eddy current. Cracks due to severe corrosion were found just forward of BS640 and outside the area of severe corrosion determined visually and by eddy current, while the left-hand DAIS image in figure 5 clearly shows corrosion pillowing just forward of BS640.

F28-1000 service aircraft

The F28-1000 lap splice sample was a strip 165 cm long containing about 200 rivets. The sample had been removed from the location shown in figure 1, owing to excessive *externally* visible corrosion. This had previously led to the lap splice outer sheet being “cleaned up” to a depth of about 0.25 mm, reducing the sheet thickness from 1.2 mm, figure 3, to less than 1 mm. The lap splice was disassembled and examined by the NLR for cracks. The procedure is given in table 3.

Table 3 F28-1000 lap splice sample disassembly and examination for cracks

<ul style="list-style-type: none">• Macroscopic/mesosopic<ul style="list-style-type: none">• drilling out rivets and lap splice disassembly• chemically stripping the paint and primer layers, followed by cleaning• visual examination (50 × binocular) of outer sheet surfaces• eddy current non-destructive inspection of outer sheet rivet holes• opening-up selected outer sheet rivet holes by tensile testing 3.5 cm × 1 cm wide vertical strips, each containing a rivet hole in an area that had undergone severe <i>external</i> corrosion• visual screening (50 × binocular) for fracture surface appearances• Mesoscopic/microscopic<ul style="list-style-type: none">• no actions (see text)

Eddy current non-destructive inspection was done with a Nortec 3551F pencil probe and Nortec 19 E2 equipment operating at 100 kHz. No crack indications were obtained. The subsequent



tensile tests showed only overload failures, i.e. no evidence of any pre-existing cracks. Consequently no mesoscopic-to-microscopic examination was done.

The results were unexpected, since the location of the lap splice sample is known to be MSD-susceptible. In fact, a 450 mm long MSD crack was found in the same aircraft at the same location on the left-hand side of the pressure cabin. From these results we may draw two conclusions:

- (1) Excessive external corrosion in an MSD-susceptible area need not be associated with fatigue cracking, despite stress increases in the lap splice outer sheet owing to cleaning up and thinning it.
- (2) Even in an MSD-susceptible area it is possible to accumulate many flights (34,470 , see table 1) without fatigue crack initiation.

FATIGUE

Fatigue assessment was to determine the MSD locations, any environmental (corrosion) influences on fatigue crack initiation and growth, crack initiation lives and early crack growth rates. The F28-4000, F100 and BAC 1-11 lap splice samples were macroscopically examined before being disassembled. As expected (6), the most MSD-susceptible rivet row in each sample was the upper one in the outer sheet. However, other rivet rows were also susceptible, notably the lower one in the inner sheet, see figure 2.

Observational aspects of early MSD

Table 4 lists the observational aspects of early (small crack) MSD for pressure cabin longitudinal lap splices. The qualification “small” means crack sizes less than 5 mm. Beyond this the crack front shapes are of less interest. Also, and more importantly, the cracks will eventually link up, possibly resulting in fracture surface damage and obscuration owing to out-of-plane movement.

The most significant general aspect of table 4 is the distinction between fatigue initiation and crack growth. It is physically incorrect to assume, as is often done by damage tolerance analysts, that fatigue is a regular crack growth process beginning during the first load cycle.



MSD fatigue initiation characteristics

Figure 11 shows the characteristic MSD fatigue crack locations and shapes in the F28-4000, F100 and BAC 1-11 lap splice samples. These will be discussed separately, followed by a summary.

- (1) F28-4000 service aircraft: The total lengths of MSD were 530 mm and 330 mm for aircraft [1] and [2] respectively. The fatigue cracks initiated at numerous sites along the faying surface edges of the outer sheet dimpling cones, see figures 3 and 11. The cracks were mechanically induced: there was no evidence that corrosion played a role in initiation. The large number of initiation sites (many cracks initiating at each dimpling cone) suggests that fatigue cracking began soon after the aircraft entered service.
- (2) F100 full-scale test (indoors): The MSD extended over several frame bays having poor adhesive bond quality. The fatigue cracks initiated from the faying surfaces, mostly at multiple sites close to the rivet holes, see figure 11. There was no evidence of corrosion, as expected from a test indoors.
- (3) BAC 1-11 service aircraft: Two sections, port and starboard, of lap splices suspected to contain MSD were disassembled and the rivet holes *carefully* opened up (4). The MSD was found along about 500 mm of the lap splices. The fatigue cracks initiated at a variety of locations, see figure 11, though mainly at faying surfaces close to the rivet holes (types A, C and D). There was no evidence that corrosion played a role in initiation.

In summary, bearing in mind that the F28 dimpled lap splices are uncustomary, the investigation of in-service and full-scale test MSD showed that fatigue initiation occurred mostly from faying surfaces near or at the rivet hole corners. This means that the faying surface condition (cladding, anodising, priming, interfay sealant, adhesive bonding) and rivet hole corner quality are very important. Also, fretting must play a role, if not always during crack initiation, then probably during early crack growth (7).

Secondary fatigue initiation characteristics: B 727-100 service aircraft

Figure 11 also shows the secondary fatigue crack locations and shapes in the B 727-100 cracked lap splice. Twelve small fatigue cracks were found at seven rivet hole locations, see figures 7 and 8. As mentioned earlier, these cracks showed no evidence of fatigue initiation due to local corrosion (pitting). Ten of the cracks, types A and B in figure 11, occurred inside the rivet holes



in the inner sheet. This behaviour appears to be distinct from MSD, where the majority of fatigue cracks initiated from faying surfaces, as was also found in a separate investigation (8).

Early fatigue crack growth: environmental effects

Unlike fatigue initiation, there was evidence that the fatigue fracture surfaces from service aircraft had been affected by the local environments, either by post-cracking corrosion or during crack growth. The MSD and secondary fatigue fracture surfaces from the F28-4000, BAC 1-11 and B 727-100 service aircraft all showed varying amounts of post-cracking corrosion. This partially obscured the fractographic characteristics, for example making it difficult to measure fatigue striation spacings near the crack initiation sites. However, on the whole it may be concluded that the local environments within the lap splices had only mild effects on the fatigue fracture surfaces: if this were not so, then the fracture surfaces would have been obliterated by substantial buildups of corrosion products (9).

Of more interest are any effects of the local environments during fatigue crack growth. Evidence for such effects was observed, as follows:

- (1) Figure 12 shows a particularly clear example of fracture surface “beach marks”. These sometimes occurred during early MSD crack growth in the F28-4000 and BAC 1-11 lap splices, and were usually present on the secondary fatigue fracture surfaces from the B 727-100 lap splice. The beach marks could well indicate periodic changes in the local environment (10). At least for the F28-4000 aircraft, it is certain that the beach marks were *not* due to variable amplitude loading, since the pressure cabins of these aircraft were subjected to the maximum pressure differential in each flight. Also the lap splice sample position, see figure 2, would not have been sensitive to gust loads.

Additional evidence is provided by figure 13, which shows the effect of changing from “dry” to “wet” air on the fatigue fracture behaviour of 2024-T3 cycled at a low frequency of the same order as in-service cabin pressure cycling, and at overall crack growth rates similar to those for early crack growth in the lap splices (see below).

- (2) Figure 14 shows a secondary fatigue fracture surface from the B 727-100 lap splice, with special features (arrowed) similar to those found – albeit more abundantly – for corrosion fatigue at low stress intensities, figure 15.

At present the significance of these observations, other than being diagnostic for environmental fatigue crack growth, is somewhat limited (more work needs to be done). Fatigue striation

spacing measurements for the light and dark bands comprising the beach marks have to date shown no systematic differences in crack growth rates (12). This could mean that modelling and prediction of early MSD crack growth need not account for environmental effects over and above that of normal air.

By comparison with data in Ref. (9) the special features of secondary fatigue fracture in the B 727-100 lap splice suggest crack growth rates below 10^{-8} m/cycle. However, the fatigue striation spacings for the crack shown in figure 14 appeared (rather vaguely, owing to corrosion) to be more than $0.1 \mu\text{m}$, implying crack growth rates above 10^{-7} m/cycle. The reality of this “discrepancy” has not yet been checked, but it is much less important than the determination of early MSD crack growth rates.

Early MSD crack growth rates

(1) Transverse (through-thickness) crack growth rates: Observation of transverse fatigue crack growth near the rivet holes was usually hampered by fretting products and, in the case of service aircraft, fracture surface corrosion. Figure 16 shows NLR and Fokker data from fatigue striation measurements on comparatively clean and undamaged fracture surfaces. Also shown is an estimate for the F100 test at 100 % design load. This estimate is obtained from the factor $(100/110)^{7.1}$, where 7.1 is the “Paris Law” exponent in a piecewise linear fit to $\log da/dN$ versus $\log \Delta K$ data for 2024-T3 in the same range of crack growth rates. There are two noteworthy features in figure 16:

- The data and estimate are well above 10^{-8} m/cycle.
- The through-thickness crack growth rates were more or less constant for each aircraft.

These features will be discussed further in the next section, MSD fatigue modelling and simulation.

(2) Longitudinal crack growth rates: Figure 17 summarises NLR, Fokker and NASA data obtained from fatigue striation and marker band measurements for the F100, BAC 1-11 and a Boeing aircraft, together with an estimate for the F100 test at 100 % design load, as discussed above. The NLR and Fokker data are presented more fully in Refs. (13, 14). There are two noteworthy features in figure 17:

- The data and estimate are above 10^{-8} m/cycle.

- The crack growth rates for different aircraft types are fairly similar in the range of crack sizes from 0.5 mm to 2mm. This is remarkable in view of the differing joint designs, see figure 3 and Ref. (12).

As before, these features will be discussed further in the next section, MSD fatigue modelling and simulation.

MSD FATIGUE MODELLING AND SIMULATION

General remarks

The fatigue behaviour of pressure cabin longitudinal lap splices is determined by complex load and stress distributions that are very difficult to analyse (6, 14, 15). In particular, this means realistic stress intensity factor solutions are not available for cracks with dimensions less than the sheet thicknesses: and one may doubt the usefulness, through lack of accuracy, of solutions for cracks with dimensions less than the rivet hole diameters.

Nor does it seem possible to model fatigue initiation by analysis. This is not only because of the complex stress fields, but also because MSD fatigue initiation in lap splices depends strongly – if not totally – on the local behaviour of various materials (aluminium alloy matrix, cladding and anodising layers, primers and sealants) at the faying surfaces and near or at rivet hole corners (14, 16). Note, in passing, that models based on fatigue initiation at corrosion pits (17) or inclusions (18) are most probably irrelevant and anyway too simple for 2024-T3 Alclad lap splices: the F28-4000 and BAC 1-11 service aircraft samples showed no evidence of corrosion pitting, and tests have shown time and again that fatigue cracks initiate in the cladding, not the 2024-T3 matrix (4, 16, 19, 20).

Instead, and at least for the present, recourse must be made to empirical modelling that describes the *actual early MSD fatigue behaviour* of lap splices from service aircraft and full-scale test articles. One such model, due to Eijkhout (13), is described and illustrated next.

Empirical model for crack growth and determination of crack growth and crack initiation lives

Eijkhout's model is based on the following observations:

- (1) MSD fatigue cracks tend to initiate at several sites near or at rivet hole corners and grow in directions varying gradually from transverse to longitudinal, see figure 18.



- (2) The transverse (through-thickness) fatigue crack growth rates are nearly constant, e.g. figure 16.
- (3) The transverse and longitudinal fatigue crack growth rates are similar for cracks with dimensions less than twice the sheet thickness, compare figures 16 and 17 (sheet thicknesses 1.2–1.3 mm, see figure 3).

Figure 19 is a schematic of the model. There are three main assumptions, the first two being derived from the foregoing observations. These assumptions are:

- Constant crack growth rate in the transverse direction, in general equal to the *initial* crack growth rate in the longitudinal direction, i.e. $dc/dN = Ae^{Ba_i}$.
- Crack depth $c = 0$ at a_i , the “initiation length”.
- Quarter-circular crack fronts in the transition from transverse to longitudinal crack growth.

These assumptions are convenient but not essential. For example, the model can be used for non-constant dc/dN and for crack initiation at rivet hole corners, i.e. $a_i = 0$ in figure 19. Also the model can be used for both non-countersunk and countersunk lap splice sheets.

Figure 20 gives examples of the model’s use. It is seen that besides providing estimates of the fatigue crack growth lives and hence the fatigue initiation lives, the model also enables estimates of the lives at which cracks become through-thickness. This information is potentially useful for in-service non-destructive inspection.

Another interesting point is that the model can be made compatible with marker bands on the fatigue fracture surfaces of full-scale test articles, as in the case of the Boeing aircraft (8). When determining the striation-based crack growth rate equations, $da/dN = Ae^{Ba}$, for individual cracks one can check the equations’ compatibility with the distances between marker bands, adjusting the equations if necessary.

Fatigue initiation lives

Table 5 gives estimates of the MSD fatigue initiation lives for the three types of aircraft in the present investigation and the Boeing aircraft (8) mentioned earlier. The F28-4000 estimate is no more than a reasonable guess. The F100 and BAC 1-11 estimates were obtained using Eijkhout’s model (13). The Boeing aircraft estimates were made from marker band analyses (8).



Table 5 Estimates of MSD fatigue initiation lives in fuselage longitudinal lap splices

Aircraft type	MSD rivet row	Lives to first crack initiations	
		Flights	Simulated flights
F28-4000	outer sheet upper row	a few thousand?	
F100	outer sheet upper row		60,000
	inner sheet lower row		70,000
BAC 1-11	outer sheet upper row	60,000	} @ 110 % design load
	inner sheet lower row	50,000	
Boeing aircraft	outer sheet upper row		5,000–15,000 @ 100 % design load

Table 5 shows there is considerable variation in the estimated fatigue initiation lives, although the F28-4000 lap splices are not of general interest. Actually, the total variation is greater: for the F100 full-scale test the estimates ranged from 60,000 – 97,000 simulated flights, and for the BAC 1-11 the estimates ranged from 50,000 – 74,000 flights.

Fatigue crack growth behaviour

From the sub-section of this paper on early MSD crack growth and figures 16 and 17 it is apparent that the transverse and longitudinal fatigue crack growth rates were above 10^{-8} m/cycle for crack sizes ranging from 30 μ m to 5 mm. This result has to be compared with figure 21, which shows the short and long fatigue crack growth behaviour of 2024-T3 for two stress ratios covering the range to be expected in fuselage longitudinal lap splices (15). Figure 21 shows that at crack growth rates above 10^{-8} m/cycle there is only long crack growth behaviour. In other words, one should not expect any difference between short and long fatigue crack growth behaviour in fuselage longitudinal lap splices, which facilitates crack growth modelling.

However, the relatively high early crack growth rates in actual fuselage longitudinal lap splices make questionable the usefulness and relevance of sub-scale specimen tests. Uniaxial specimens “simulating” the F100 fuselage longitudinal lap splice had early crack growth rates far too low compared with the full-scale test results (22). This was also true for biaxial specimens (23). This situation may change when improved stress analyses become available and are used for improving sub-scale specimen design and testing. On the other hand, it may turn out that reliance will still have to be made mainly on full-scale fuselage section or panel tests (24, 25).



DISCUSSION

Lap splice corrosion and fatigue in service aircraft

Severe internal corrosion in a B 727-100 lap splice and external corrosion of an F28-1000 lap splice did not lead to MSD fatigue crack initiation. However, the B 727-100 lap splice had small, secondary fatigue cracks. These usually initiated from intergranular cracks due to corrosion and stress corrosion, but sometimes occurred directly from rivet holes, without any evidence of fatigue initiation due to local corrosion (pitting). Twelve of the latter type of cracks were located at seven rivet holes without any corrosion-induced cracking. These cracks most probably initiated owing to a combination of normal in-service stresses and additional stresses caused by corrosion product buildup (pillowing) between the outer and inner sheets of the lap splice.

Examination of MSD fatigue cracking in lap splices from three service aircraft, two F28-4000s and a BAC 1-11, also showed no evidence of fatigue initiation due to local corrosion. Thus it would appear that pressure cabin longitudinal lap splices have either a corrosion problem or a fatigue problem, i.e. there is no *primary* association between corrosion and fatigue.

There was, however, evidence of local environmental effects during early fatigue crack growth. For MSD the environmental effects on crack growth rates were mild, if any. It is as yet uncertain whether the fatigue crack growth rates in service would be significantly different from those determined by testing in normal air.

Lap splice fatigue analysis

(1) Analysis methods: Figure 22 shows the “traditional” and developing fatigue analysis methods for transport aircraft fuselage lap splices:

- In the “traditional” methods the inspection threshold is established using fatigue life S-N data, cumulative linear damage analysis (if deemed necessary) and scatter factors. Subsequent inspection intervals are based on a safe fatigue crack growth period using da/dN versus ΔK_{eff} long crack growth data, crack growth models for spectrum loading (if deemed necessary) and scatter factors.
- In the developing methods the inspection threshold is intended to be established using fatigue crack growth analysis and tests, whereby it is assumed the structure contains initial flaws (Initial Quality Flaw Sizes, IQFS). Subsequent inspection intervals are

based on a safe fatigue crack growth period that accounts for MSD essentially as a refinement – however important – to the “traditional” analyses.

- (2) Analysis problems of actual versus predicted behaviour: Figure 23 is a schematic of the likely differences between actual early MSD crack growth behaviour, as described in the present paper, and predictions using macroscopic (long) crack growth modelling, whereby the IQFS values are obtained either from actual data for manufacturing flaws or by back-extrapolation using a long crack growth model.

For both types of prediction the long crack growth model is used to make an empirical fit such that the fatigue life is represented as a continuous crack growth process, beginning as soon as the aircraft enters service. This premise is incorrect: crack initiation is a physical reality. The fitted model therefore has limited transferability, and in general should not be used for “blind” predictions of crack growth in other structural areas with differing lap splice geometries and – most importantly – differing faying surface conditions. Nor should the fitted model be used for predicting crack growth at different (local) stress levels. This latter point is significant for two reasons:

- The stress-dependence of fatigue initiation life will probably be very different to that of fatigue crack growth, e.g. Ref. (26).
- Actual fatigue crack growth rates could be in a different “Paris Law” regime, i.e. the exponent m in the relation $da/dN = C(\Delta K)^m$ could be different. An example of a surprisingly high but realistic exponent, $m = 7.1$, was mentioned for transverse (through-thickness) crack growth rates and is shown in figure 21.

There would seem to be no solution to the above problems so long as it is assumed that crack growth begins as soon as the aircraft enters service. One alternative is to further investigate the usefulness of Eijkhout’s model. This possibility has much to recommend it. The model is based on physical reality: it takes account of actual lap splice fatigue initiation and crack growth behaviour, and the present paper has shown much commonality in this behaviour for several aircraft types and different positions of the lap splices. Also, as mentioned under the sub-heading of fatigue crack growth behaviour, it may turn out that fatigue crack growth analyses will have to rely mainly on full-scale fatigue testing. If so, then Eijkhout’s model provides a way of describing crack growth, notably the all-important early crack growth through the sheet thickness, and a way of estimating the fatigue initiation life. Of course, since the model is empirical, the parameters in the model have to be determined for each type of aircraft, and also – possibly – for fuselage areas where the



design stress levels are significantly different, e.g. varying by more than 10 % from the average.

CONCLUSIONS

This paper describes and discusses the characteristics of corrosion and MSD fatigue initiation and early crack growth in transport aircraft fuselage longitudinal lap splices, using examples from four aircraft types. These were a Boeing 727-100, three Fokker F28s and a British Aerospace BAC 1-11 from service, and the Fokker F100 full-scale fuselage test. Information from a NASA report on a Boeing aircraft full-scale test was also used. The following conclusions are drawn:

- (1) There is no *primary* association between corrosion and fatigue for 2024-T3 Alclad lap splices. Severe corrosion did not result in MSD, and MSD is not initiated by local corrosion. However, there was evidence of local environmental effects, albeit mild, during early fatigue crack growth in the lap splices from service aircraft. It is as yet uncertain whether the fatigue crack growth rates in service are significantly different, owing to environmental effects, from those determined by testing in laboratory air.
- (2) There was a strong tendency for MSD fatigue cracks to initiate at faying surfaces near or at rivet hole corners. However, for the severely corroded B 727-100 lap splice secondary fatigue cracks initiated usually from intergranular cracks due to corrosion and stress corrosion, but sometimes occurred directly from rivet holes without any evidence of fatigue initiation due to local corrosion.
- (3) A distinction should be made between MSD fatigue initiation and fatigue crack growth. It is physically incorrect to consider lap splice fatigue solely as a regular crack growth process that begins as soon as the aircraft enters service.
- (4) There are indications of considerable variation in MSD fatigue initiation lives, both in the range of lives for each aircraft type and between aircraft types.
- (5) The most MSD-susceptible rivet row was the upper one in the outer sheets of the lap splices. However, other rivet rows were susceptible, notably the lower one in the inner sheets.



- (6) Early MSD crack growth rates, for crack sizes 30 μm – 5 mm, were above 10^{-8} m/cycle (or flight), which means one should not expect any difference between short and long fatigue crack behaviour in the lap splices. However, the relatively high crack growth rates make questionable the usefulness and relevance of sub-scale specimen tests.

The foregoing conclusions should be taken into account during further development of fatigue analysis methods for transport aircraft fuselage lap splices.

REFERENCES

- (1) Aircraft accident report, Aloha Airlines, flight 243, Boeing 737-200, N73711, Near Maui, Hawaii, April 28, 1988, NTSB Report No. NTSB/AAR-89/03, National Transportation Safety Board, Washington, D.C., June 1989.
- (2) Gould, R.W., Komorowski, J.P., “DAIS-250C field inspections at First Air”, Report No. LTR-ST-2073, Institute for Aerospace Research, National Research Council Canada, Ottawa, September 1996.
- (3) Chapman, C.E., Fahr, A., “Nondestructive examination of aircraft lap joint specimens for the Netherlands National Aerospace Laboratory”, Memorandum LM-ST-787, Institute for Aerospace Research, National Research Council Canada, Ottawa, February 1997.
- (4) Wanhill, R.J.H., “Procedures for investigating MSD in fuselage lap splices”, Brite Euram Project No. BE95-1053, SMAAC: Structural Maintenance of Ageing Aircraft, Document No. SMAAC-TR-1.3-03-1.3/NLR, NLR Technical Report 98300, National Aerospace Laboratory, Amsterdam, July 1998.
- (5) Komorowski, J.P., Bellinger, N.C., Gould, R.W., “The role of corrosion pillowing in NDI and in the structural integrity of fuselage joints”, ICAF 97, Fatigue in New and Ageing Aircraft, Editors R. Cook and P. Poole, Engineering Materials Advisory Services Ltd., Vol. 1, pp. 251-266, Cradley Heath (1997).
- (6) Eastaugh, G.F., Simpson, D.L., Straznicky, P.V., Wakeman, R.B., “A special uniaxial coupon test specimen for the simulation of multiple site fatigue crack growth and link-up in fuselage skin splices”, Widespread Fatigue Damage in Military Aircraft, AGARD Conference Proceedings 568, Advisory Group for Aerospace Research and Development, pp. 2-1 – 2-19, Neuilly-sur-Seine (1995).

- (7) Rooke, D.P., "Fracture mechanics analysis of short cracks at loaded holes", Behaviour of Short Cracks in Airframe Components, AGARD Conference Proceedings No. 328, Advisory Group for Aerospace Research and Development, pp. 8-1 – 8-6, Neuilly-sur-Seine (1983).
- (8) Piascik, R.S., Willard, S.A., "The characteristics of fatigue damage in the fuselage riveted lap splice joint", NASA Technical Publication NASA/TP-97-206257, National Aeronautics and Space Administration Langley Research Center, Hampton, Virginia, November 1997.
- (9) Wanhill, R.J.H., Schra, L., "Corrosion fatigue crack arrest in aluminum alloys", Quantitative Methods in Fractography, ASTM STP 1085, Editors B.M. Strauss and S.K. Putatunda, American Society for Testing and Materials, pp. 144-165, Philadelphia, Pennsylvania (1990).
- (10) Darvish, M., Johansson, S., "Cyclic change in the humidity of the environment during fatigue crack propagation and its effect on fracture surface appearance", Scandinavian Journal of Metallurgy, Vol. 21, pp. 68-77 (1992).
- (11) Mussert, K.M., "Formation of beach marks on Alclad 2024-T3 sheet", Master of Science Thesis, Department of Chemical Technology and Materials Science, Delft University of Technology, Delft, December 1995.
- (12) Wanhill, R.J.H., Van der Hoeven, W., Ten Hoeve, H.J., Ottens, H.H., "Fractographic investigation of pressure cabin MSD", NLR Technical Publication 99265, National Aerospace Laboratory, Amsterdam, July 1999. To be published in ICAF'99.
- (13) Eijkhout, M.T., "Fractographic analysis of longitudinal fuselage lapjoint at stringer 42 of Fokker 100 full scale test article TA15 after 126250 simulated flights", Fokker Report RT2160, Fokker Aircraft Ltd., Amsterdam, November 1994.
- (14) Wanhill, R.J.H., "Fractography of MSD in fuselage lap splices", Brite Euram Project No. BE95-1053, SMAAC: Structural Maintenance of Ageing Aircraft, Document No. SMAAC-TR-1.3-02-1.3/NLR, NLR Technical Report 98310, National Aerospace Laboratory, Amsterdam, July 1998.



- (15) Müller, R.P.G., “An experimental and analytical investigation on the fatigue behaviour of fuselage riveted lap joints”, Delft University Press, Delft (1995).
- (16) Wanhill, R.J.H., “Effects of cladding and anodising on flight simulation fatigue of 2024-T3 and 7475-T761 aluminium alloys”, NLR Technical Report 85006 L, National Aerospace Laboratory, Amsterdam, January 1985.
- (17) Wei, R.P., Harlow, D.G., “Corrosion and corrosion fatigue of aluminium alloys – an aging aircraft issue”, Fatigue '99, Proceedings of the Seventh International Fatigue Congress, Editors Xue-Ren Wu and Zhong-Guang Wang, Engineering Materials Advisory Services Ltd., Vol. 4, pp. 2197-2204, Cradley Heath (1999).
- (18) Laz, P.J., Craig, B.A., Rohrbaugh, S.M., Hillberry, B.M., “The development of a total fatigue life approach accounting for nucleation and propagation”, Fatigue '99, Proceedings of the Seventh International Fatigue Congress, Editors Xue-Ren Wu and Zhong-Guang Wang, Engineering Materials Advisory Services Ltd., Vol. 2, pp. 833-838, Cradley Heath (1999).
- (19) Forsyth, P.J.E., “The effect of cladding condition on the stages of fatigue crack formation and growth”, Problems with Fatigue in Aircraft, Proceedings of the Eighth ICAF Symposium, Editors J. Branger and F. Berger, Swiss Federal Aircraft Establishment (F+W), pp. 2.5/1 – 2.5/23, Emmen (1975).
- (20) Schijve, J., Jacobs, F.A., Tromp, P.J., “The significance of cladding for fatigue of aluminium alloys in aircraft structures”, NLR Technical Report 76065 U, National Aerospace Laboratory, Amsterdam, July 1976.
- (21) Newman, Jr., J.C., Edwards, P.R., “Short-crack growth behaviour in an aluminium alloy – an AGARD Cooperative Test Programme”, AGARD Report No. 732, Advisory Group for Aerospace Research and Development, Neuilly-sur-Seine (1988).
- (22) Schra, L., Ottens, H.H., Vlieger, H., “Fatigue crack growth in simulated Fokker 100 lap joints under MSD and SSD conditions”, NLR Contract Report 95279 C, National Aerospace Laboratory, Amsterdam, June 1995.
- (23) Vlieger, H., Ottens, H.H., “Results of uniaxial and biaxial tests on riveted fuselage lap joints specimens”, NLR Contract Report 97319 L, National Aerospace Laboratory, Amsterdam, April 1997.



- (24) De Jong, G.J., Elbertsen, G.A., Hersbach, H.J.C., Van der Hoeven, W., “Development of a full-scale fuselage panel test methodology”, NLR Contract Report 95361 C, National Aerospace Laboratory, Amsterdam, May 1995.
- (25) Vercammen, R.W.A., Ottens, H.H., “Full-scale fuselage panel tests”, NLR Technical Publication 98148, National Aerospace Laboratory, Amsterdam, March 1998.
- (26) Schijve, J., “Fatigue life until small cracks in aircraft structures. Durability and damage tolerance”, FAA/NASA International Symposium on Advanced Structural Integrity Methods for Airframe Durability and Damage Tolerance, NASA Conference Publication 3274, Editor C.E. Harris, Part 2, pp. 665-681, Hampton, Virginia (1994).

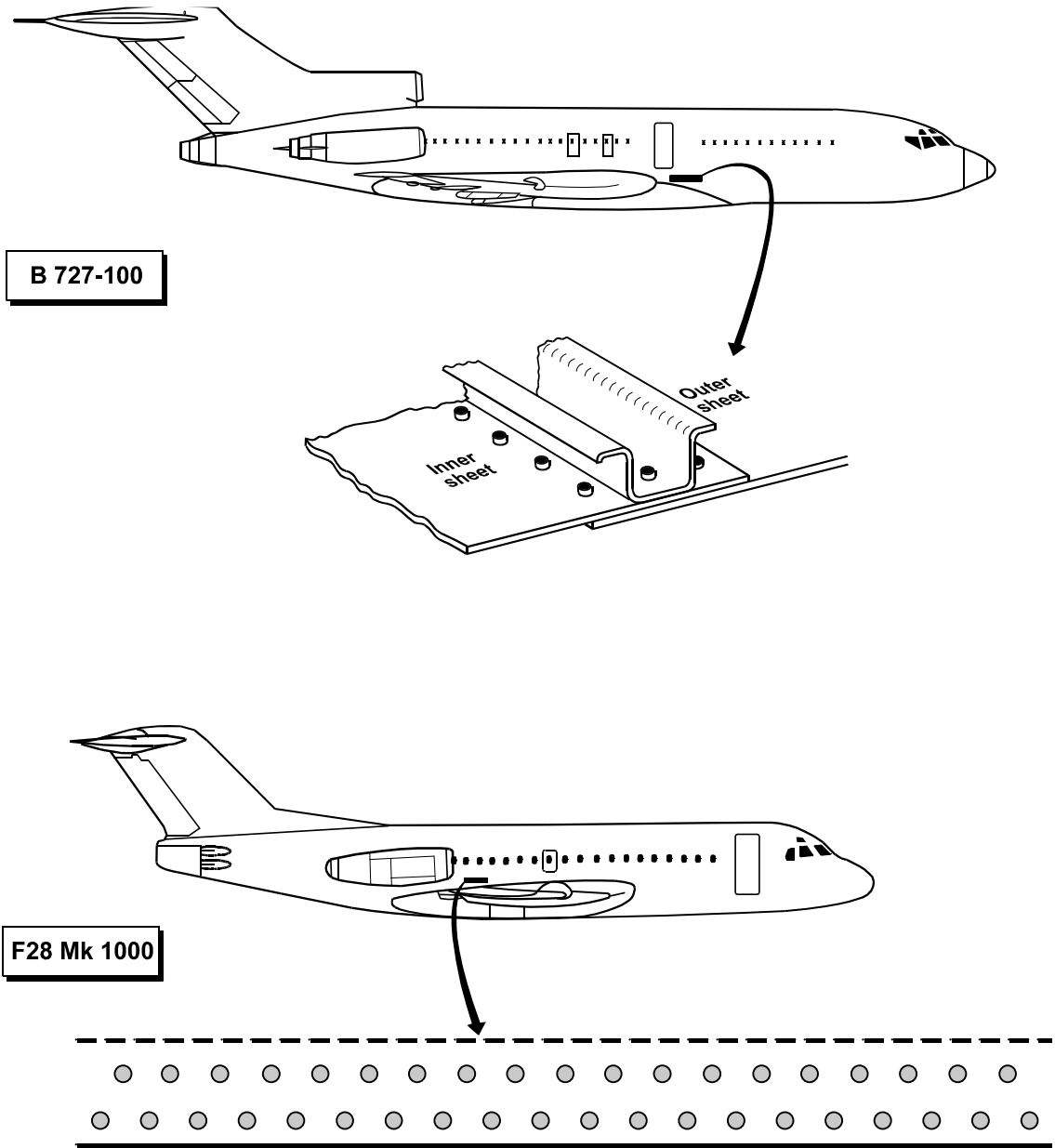


Fig. 1 Positions of the corroded lap splices

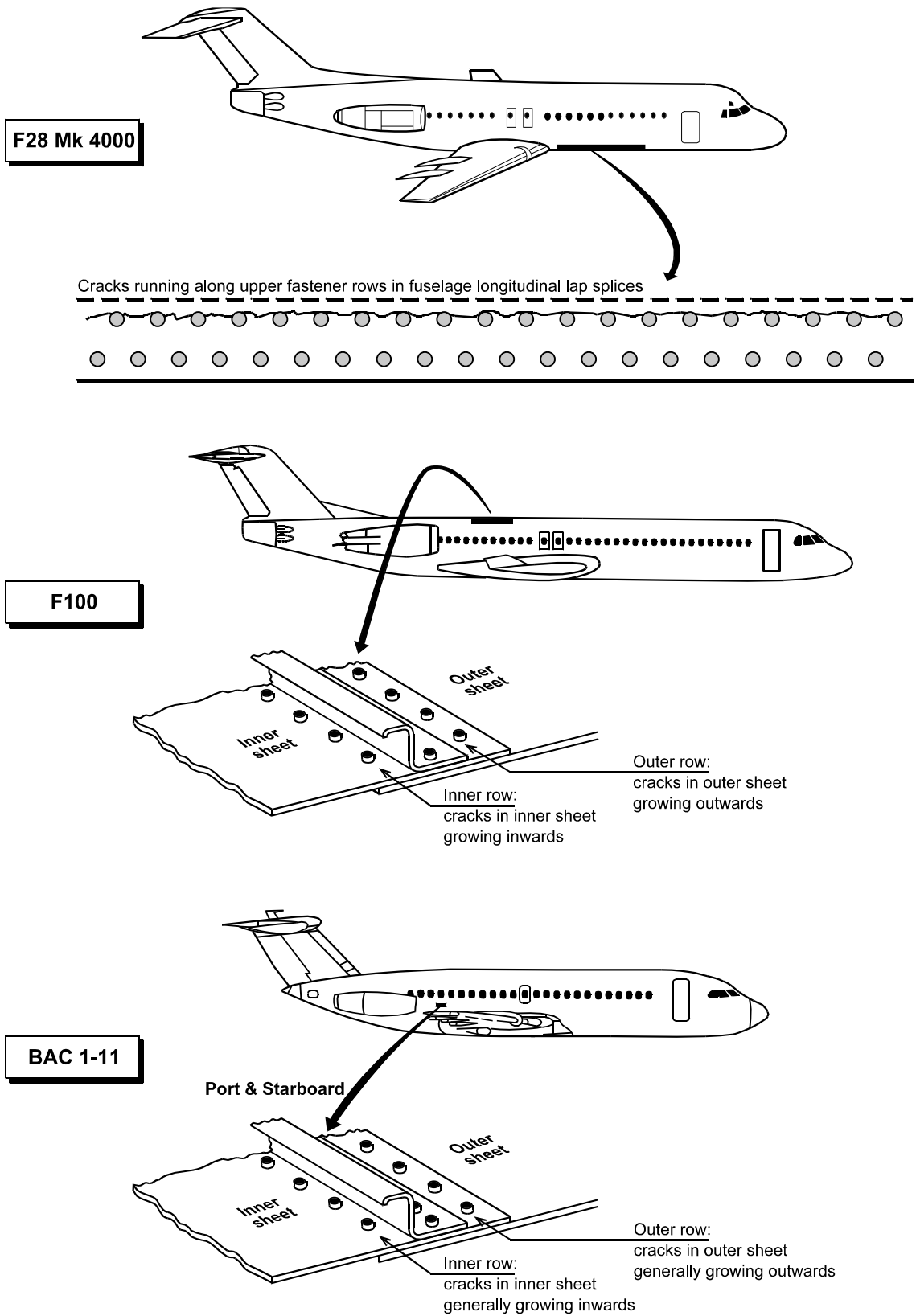
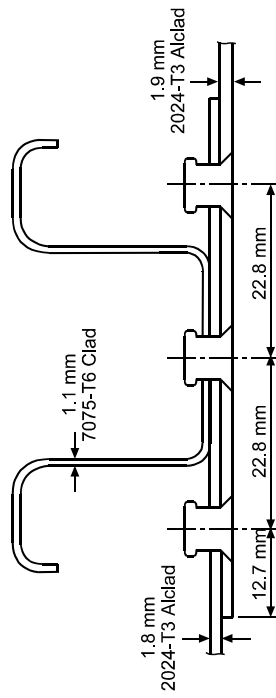


Fig. 2 Positions of the MSD fatigue cracked lap splices

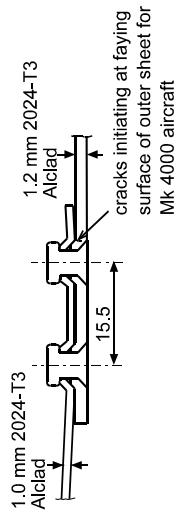
B 727-100

- rivet pitch 28-30 mm
- rivet diameter 4.9-5.1 mm
- sheets and stiffener primed
- interfac sealant



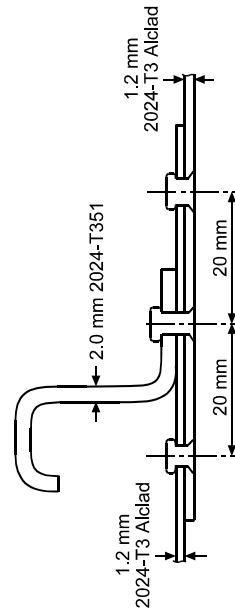
F28 Mk1000 & 4000

- rivet pitch 16.6 mm
- rivet diameter 4 mm
- sheets chromic acid anodised and primed



F100

- rivet pitch 20 mm
- rivet diameter 3.2 mm
- sheets chromic acid anodised, primed and cold bonded



BAC 1-11

- stiffener rivet pitch 12.7 mm
- sheet rivet pitch 25.4 mm
- rivet diameter 3.2 mm
- sheets chromic acid anodised and primed
- interfac sealant

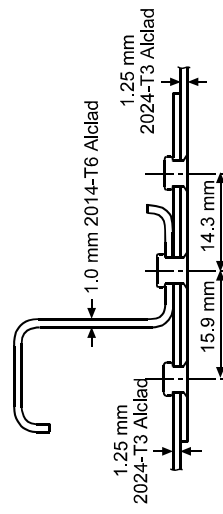
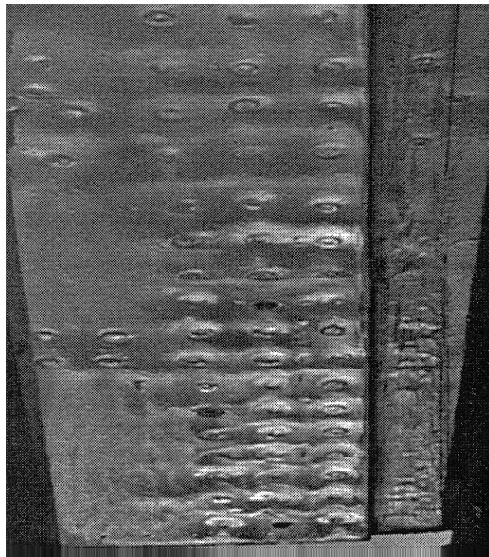


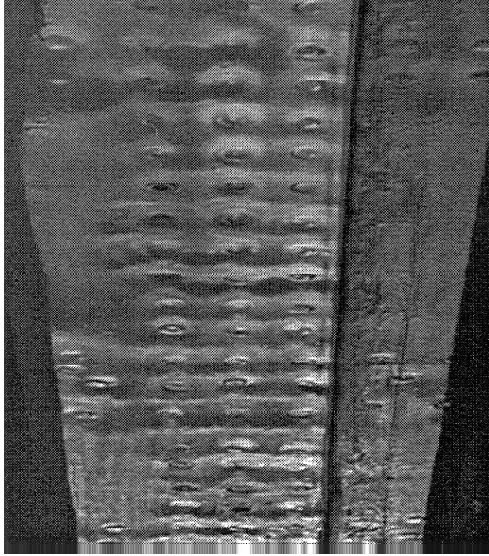
Fig. 3 Configurations of the lap splices looking FORWARD



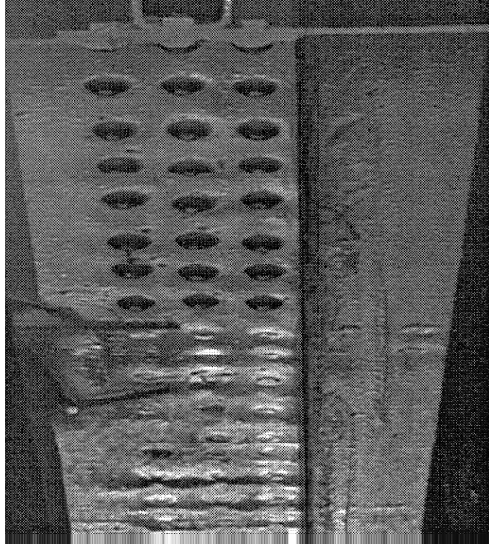
Fig. 4 Overview of the B 727-100 lap splice sample and detail of the internally visible corrosion along the upper side of the lap splice/stiffener connection



BS640



BS620



BS600

Fig. 5 DAIS imaging of corrosion-induced pilling of the B 727-100 lap splice: images courtesy of the IAR. BS = Body Station

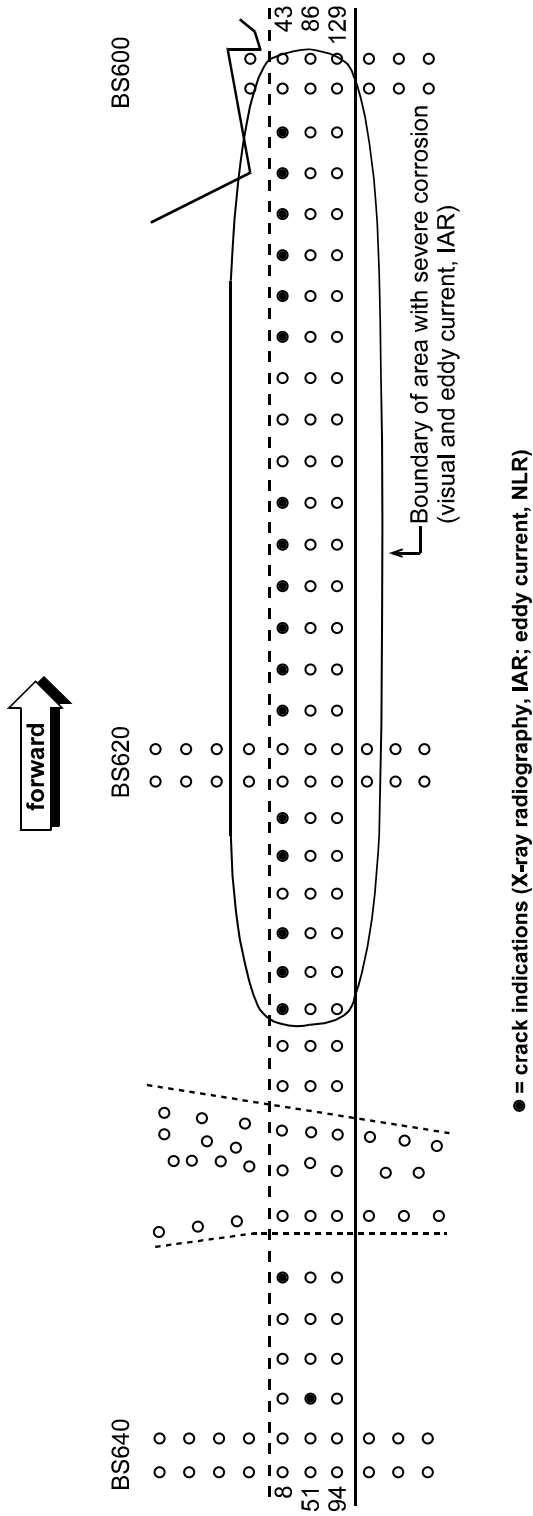


Fig. 6 Schematic of the results of the B 727-100 lap splice non-destructive inspections to determine (a) the severely corroded area, and (b) any cracking associated with rivet locations along the lap splice. The numbers at both ends of each rivet row indicate the chosen sequence of rivet numbering. BS = Body Station

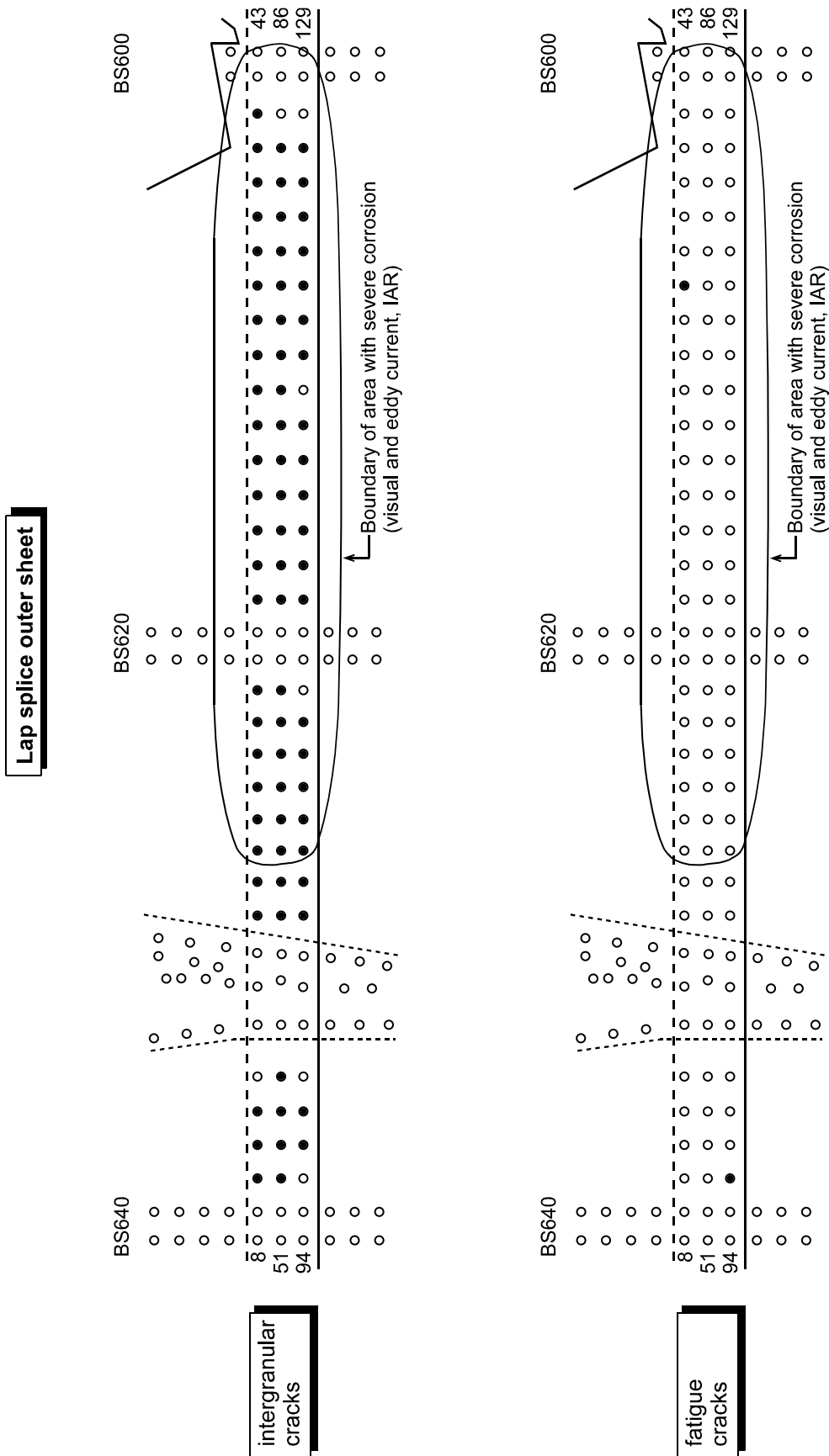


Fig. 7 Schematic of the results of the B 727-100 lap splice disassembly and examination for the outer sheet. BS = Body Station

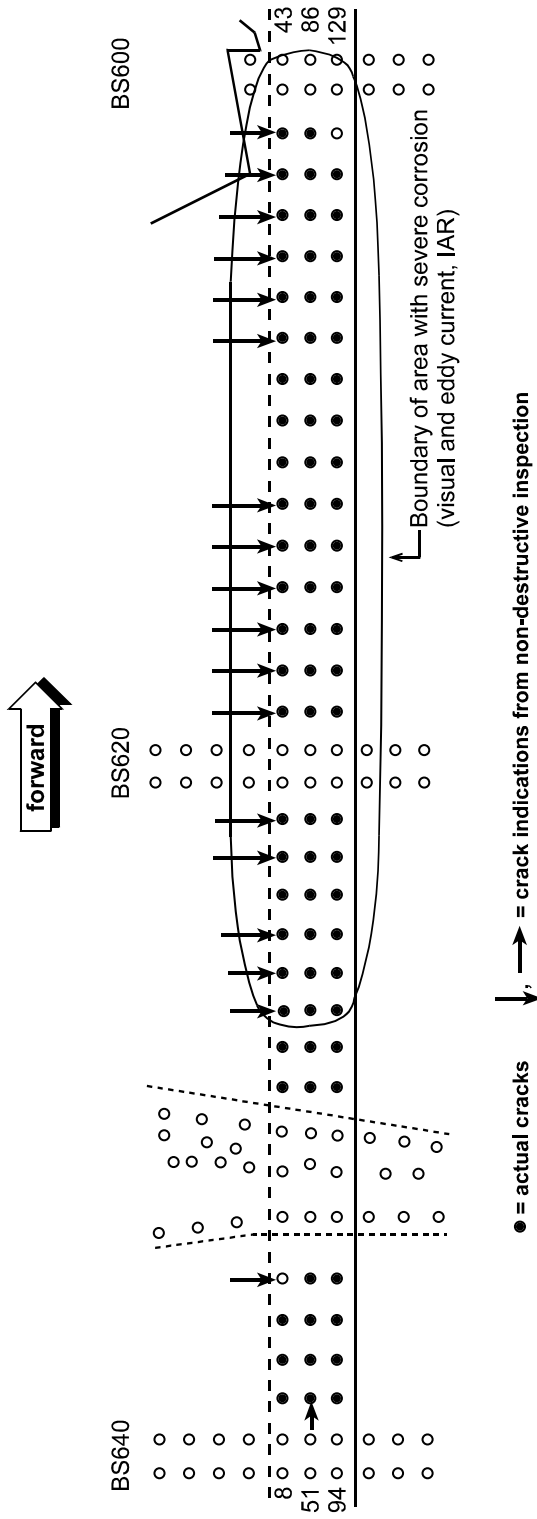


Fig. 9 Schematic comparison of the results of the B 727-100 lap splice disassembly and examination for cracks and the crack indications from non-destructive inspection. BS = Body Station

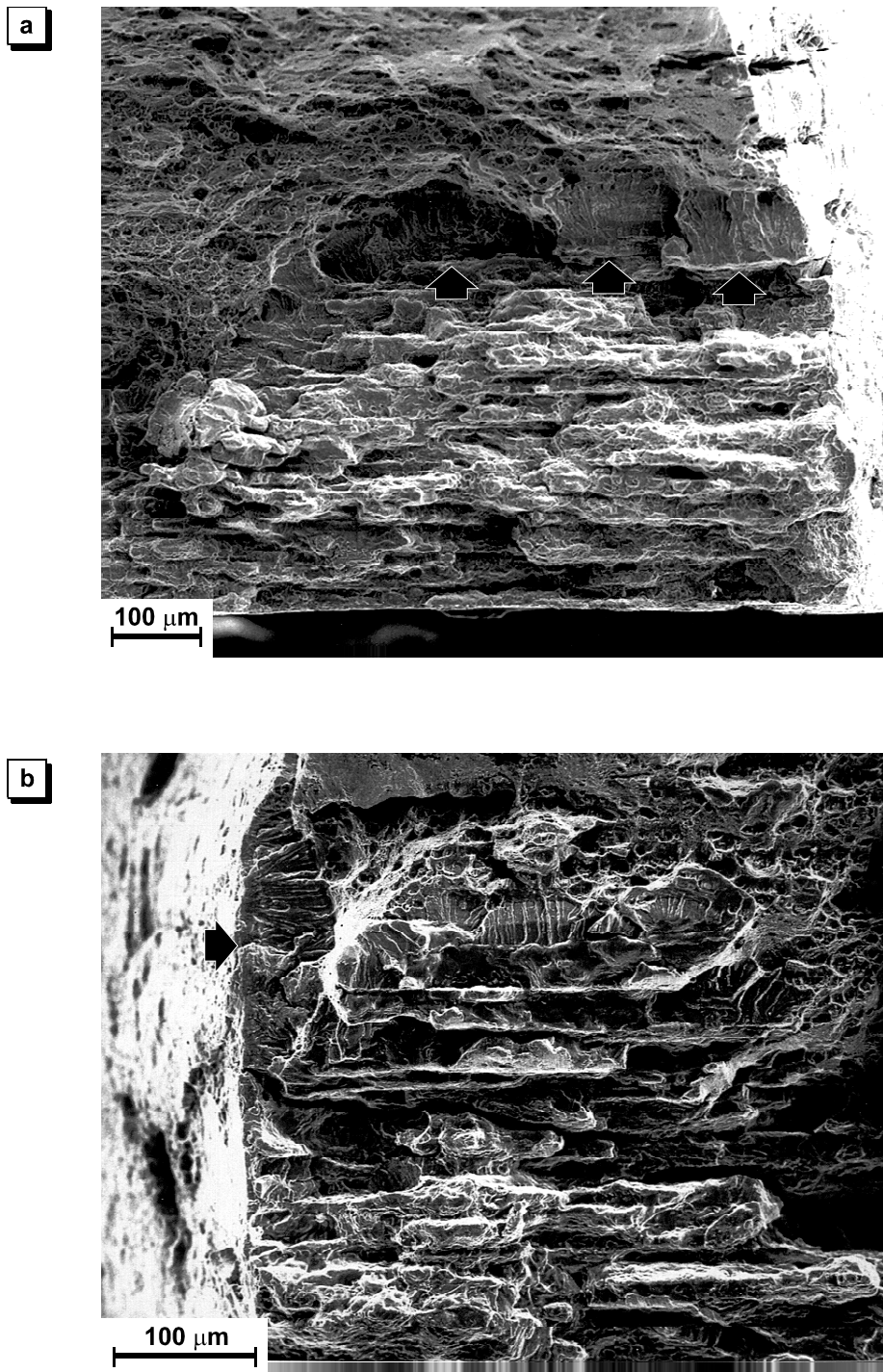


Fig. 10 Intergranular cracks with secondary fatigue cracks initiating (a) from intergranular cracking and (b) from a rivet hole: Boeing 727-100 lap splice outer sheet. Arrows point to fatigue cracks and their growth directions

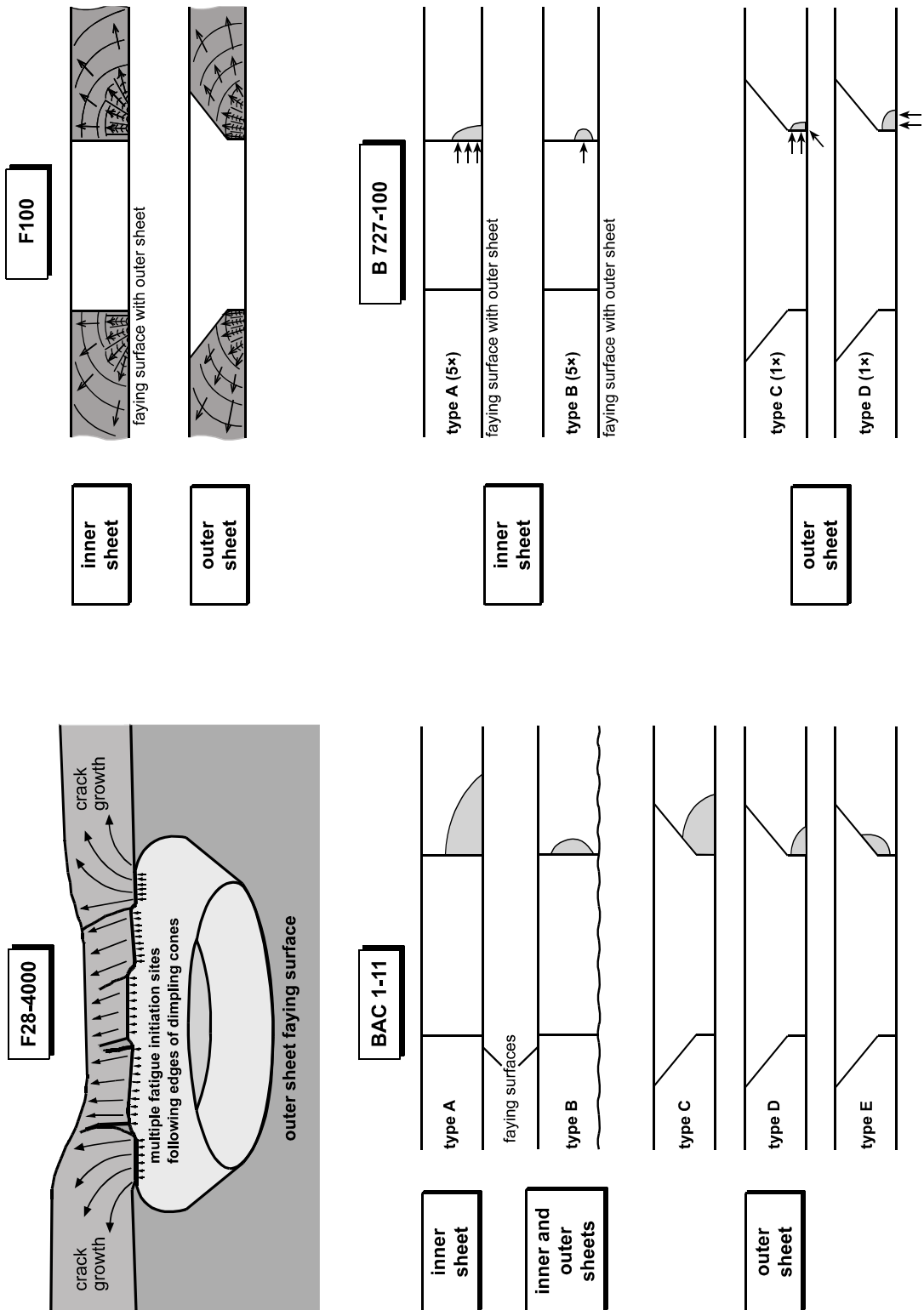


Fig. 11 MSD and secondary (Boeing 727-100) fatigue crack locations and shapes in the cracked lap splices

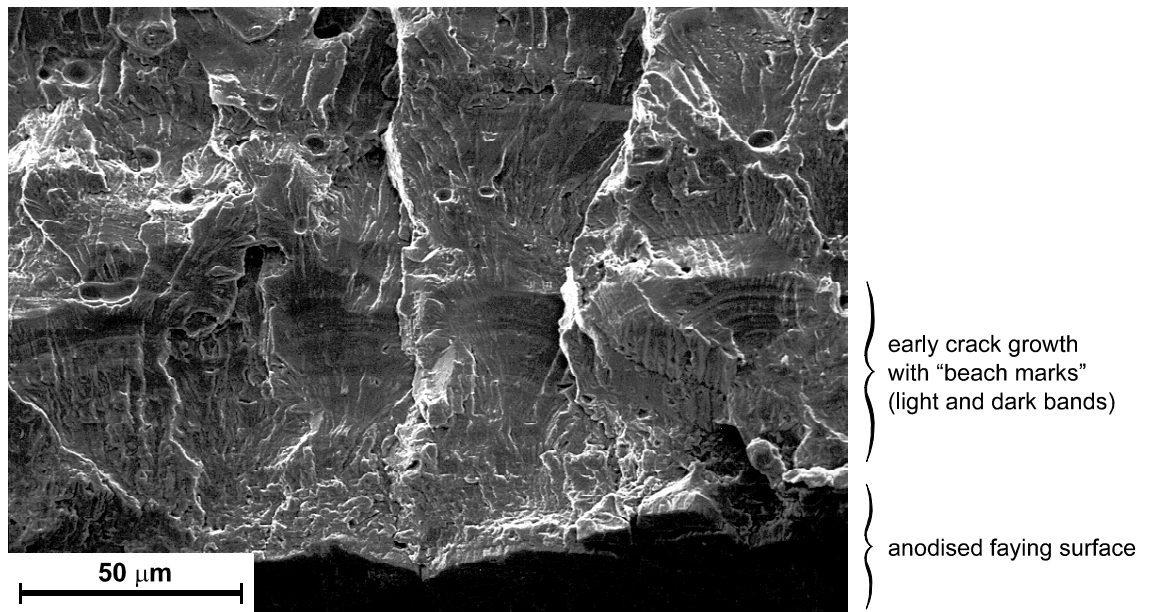


Fig. 12 Multiple site MSD fatigue initiation and early crack growth in an F28-4000 lap splice

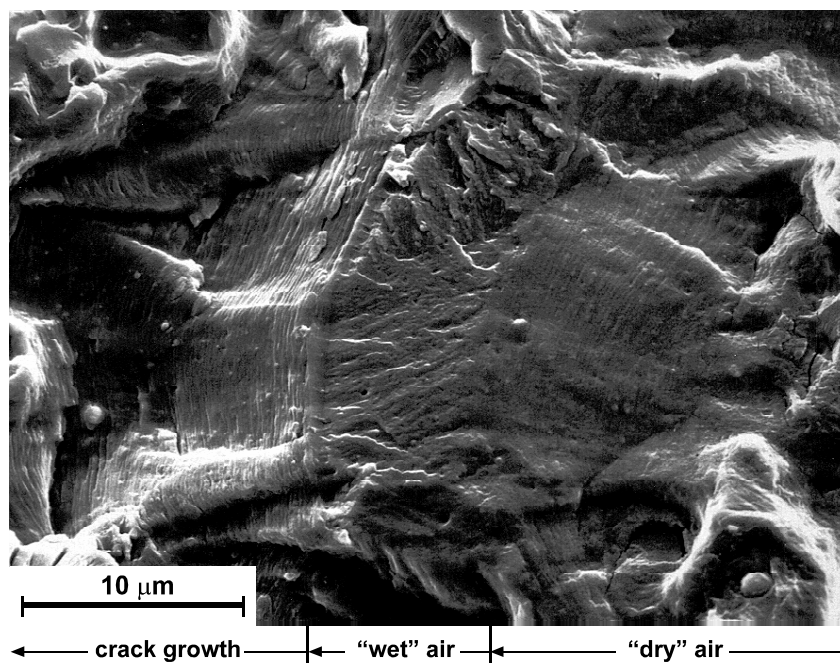


Fig. 13 Fatigue fracture topographical change for 2024-T3 cycled at 0.003 Hz in "dry" and "wet" air: $R = 0.05$, $\Delta K \sim 8.5 \text{ MPa}\sqrt{\text{m}}$ (11)

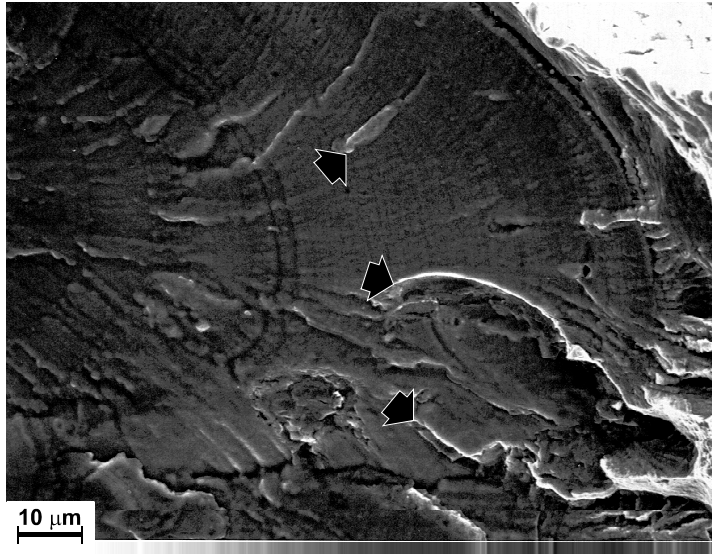


Fig. 14 Secondary fatigue crack early growth in the B 727-100 lap splice. Arrows point to narrow elliptical and semi-elliptical features with major axes in the local crack growth direction

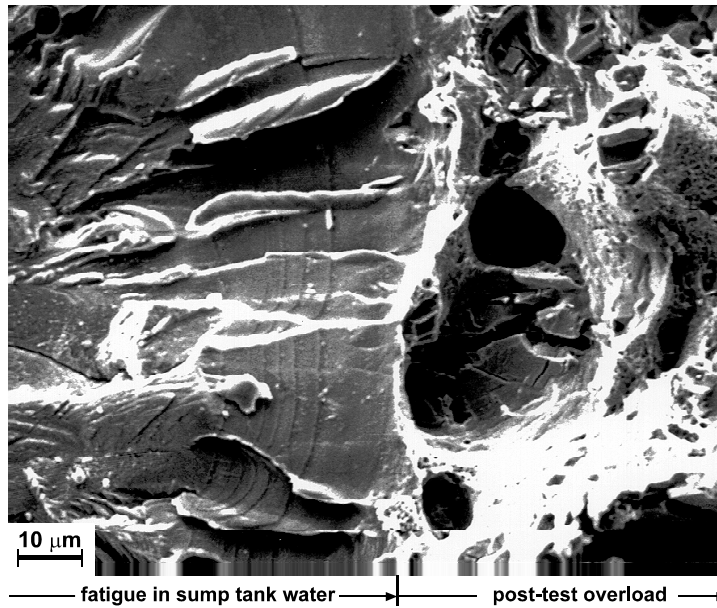


Fig. 15 Corrosion fatigue of 2024-T3 Alclad cycled at 13 Hz in sump tank water: $R = 0.1$, $\Delta K \sim 3.6 \text{ MPa} \sqrt{\text{m}}$ (9)

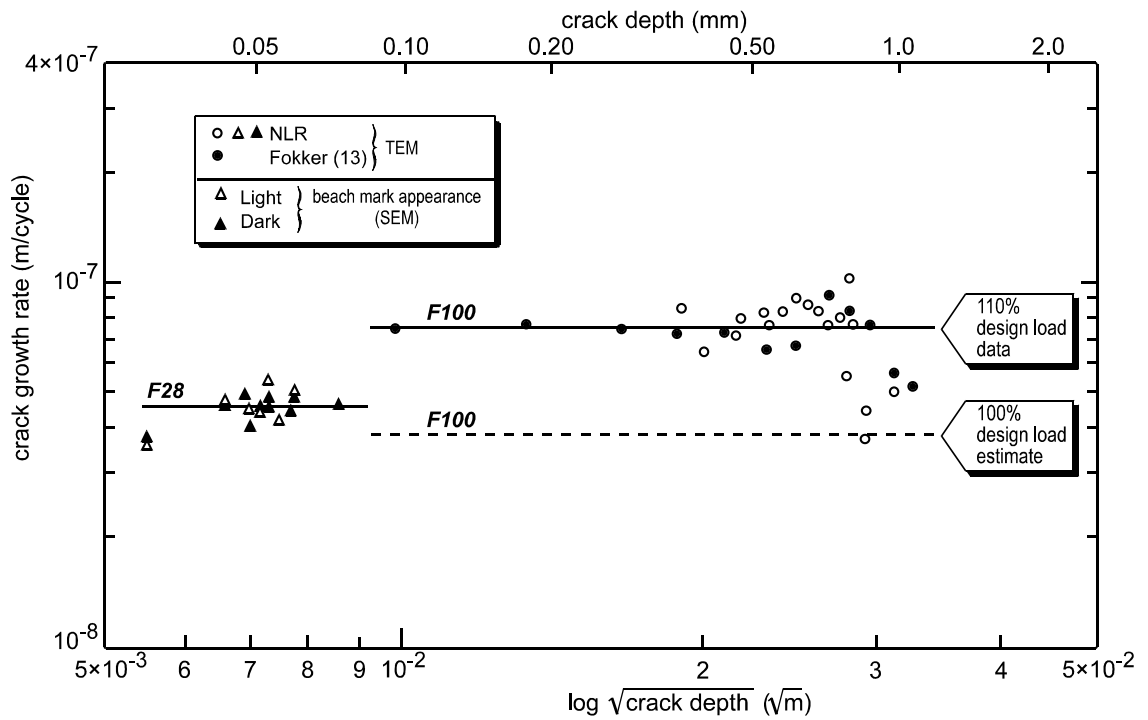


Fig. 16 Summary of transverse (through-thickness) fatigue crack growth rates: TEM = Transmission Electron Microscopy of replicas; SEM = Scanning Electron Microscopy

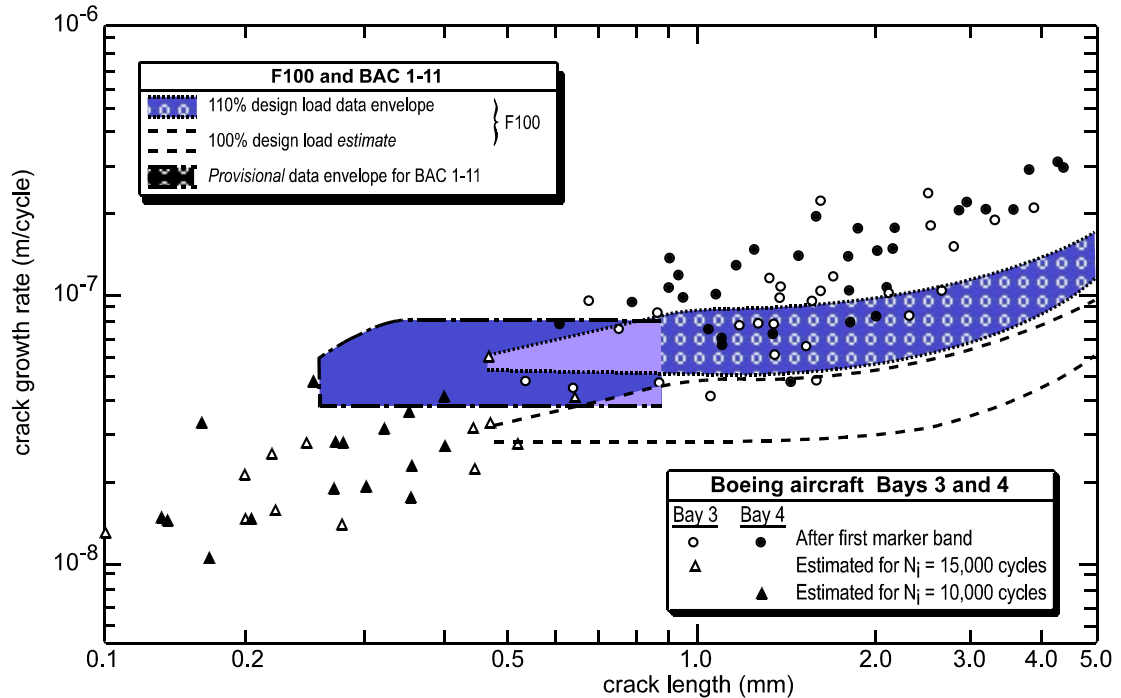


Fig. 17 Summary of longitudinal fatigue crack growth rates: Boeing aircraft data from (8)

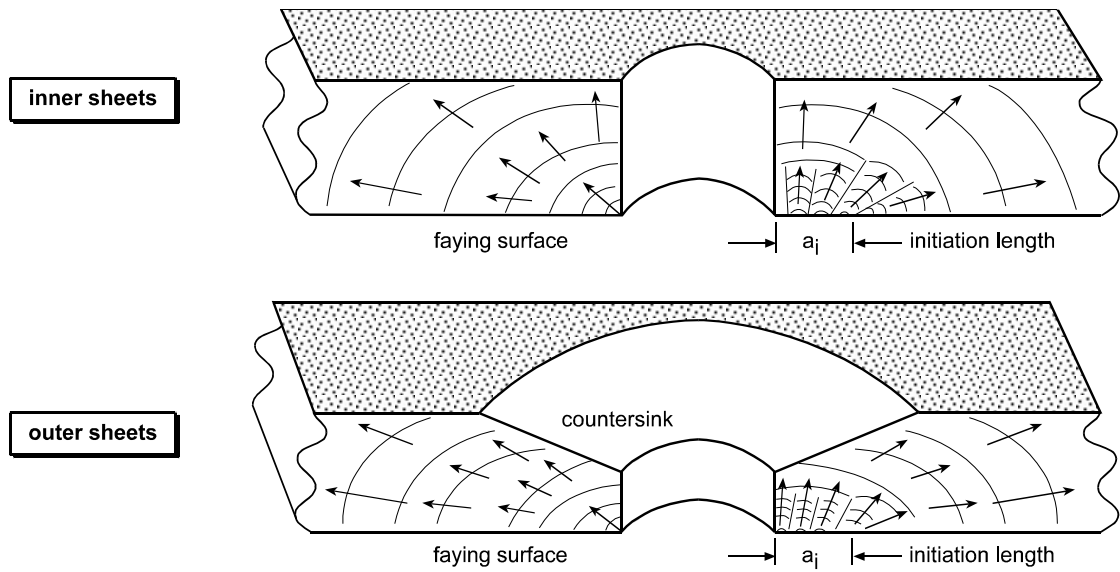
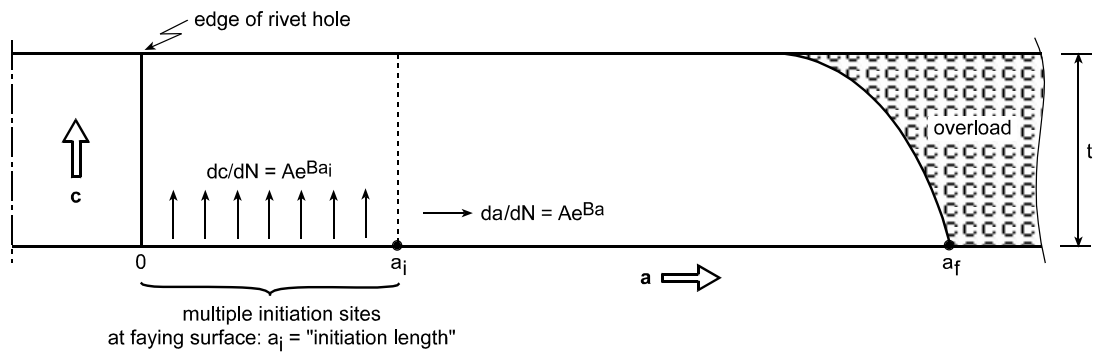


Fig. 18 Most common MSD fatigue initiation sites from service experience and full-scale testing

- From fractographic observations and striation spacings:



- a_i , a_f and N_f are known. Calculate N_i from: $N_f - N_i = \frac{1}{AB} (e^{-Ba_i} - e^{-Ba_f})$
- Calculate intermediate values of a for given values of n : $a_{int} = -\frac{1}{B} \ln [e^{-Ba_i} - AB(N_{int} - N_i)]$
- For each a_{int} calculate c_{int} from: $c_{int} = (N_{int} - N_i) Ae^{Ba_i}$
- Construct crack fronts as follows:

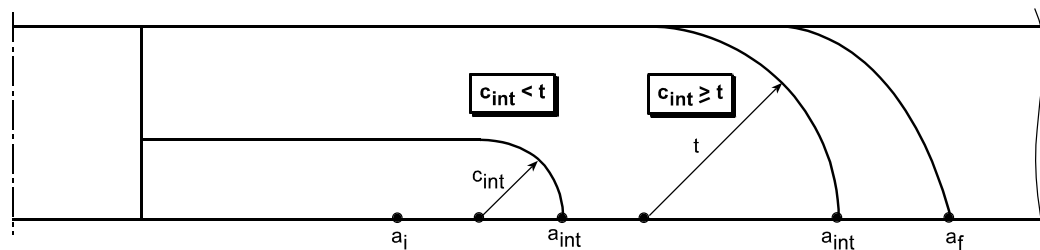


Fig. 19 Eijkhout's empirical model illustrated for a non-countersunk sheet and multiple fatigue initiation sites

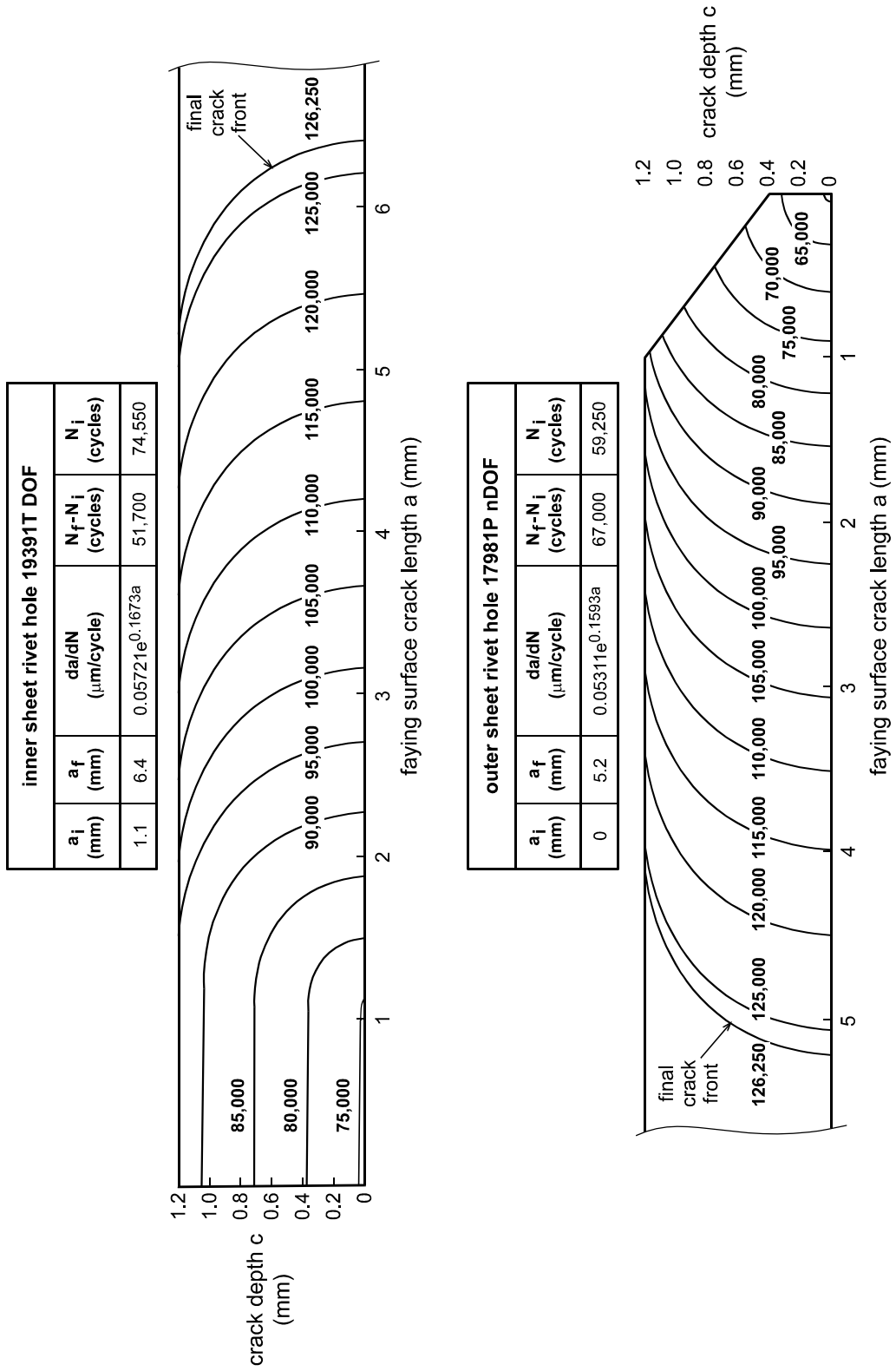


Fig. 20 Examples of the use of Eijkhout's empirical model to predict "iso-life" fatigue crack fronts for two MSD fatigue cracks in the F100 full-scale test lap splice (13): DOF = Direction Of Flight; nDOF = opposite to Direction Of Flight

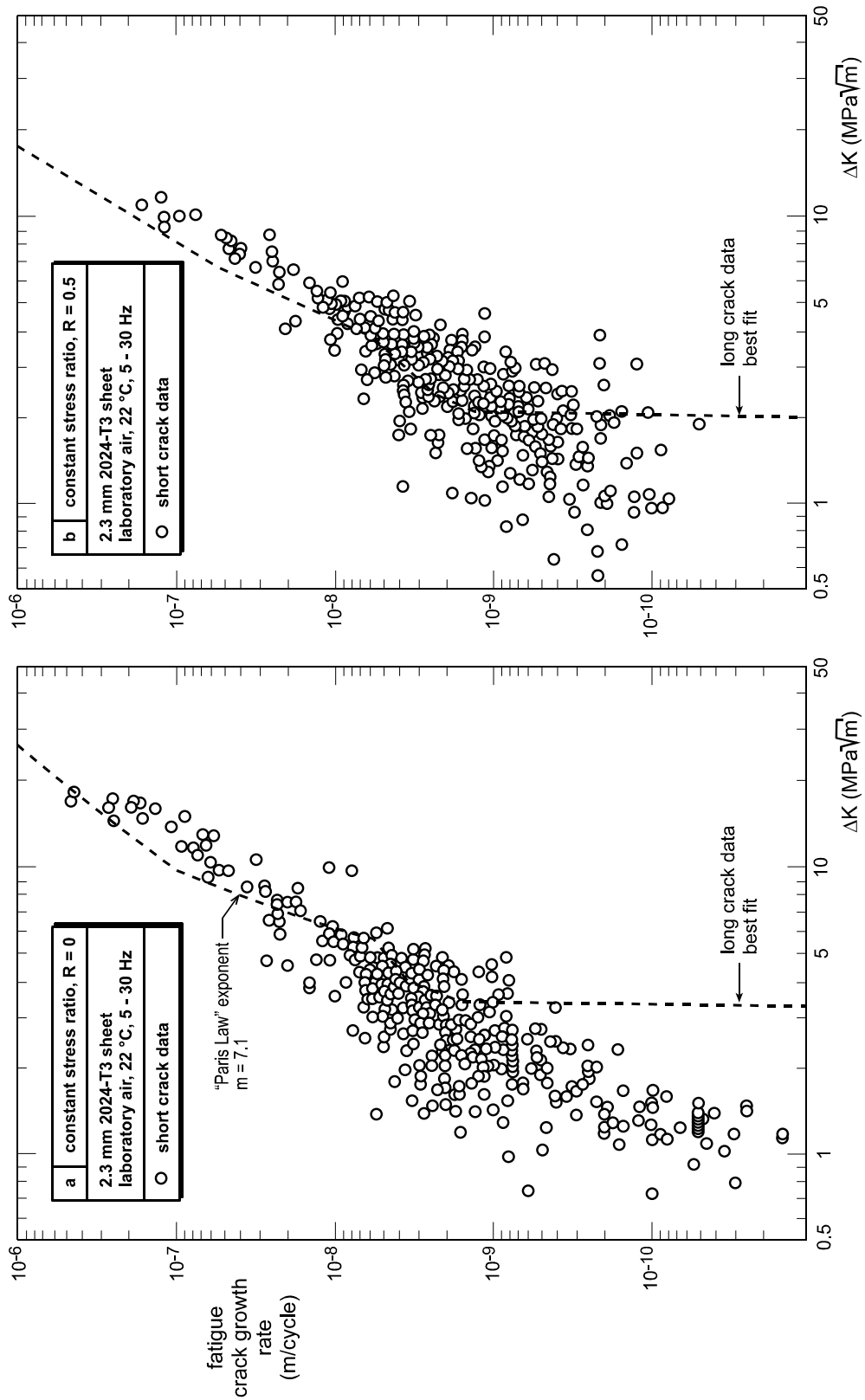


Fig. 21 Comparisons of short and long fatigue crack growth rates for 2024-T3 aluminium alloy sheet: data for specimens loaded parallel to the sheet rolling direction (21)

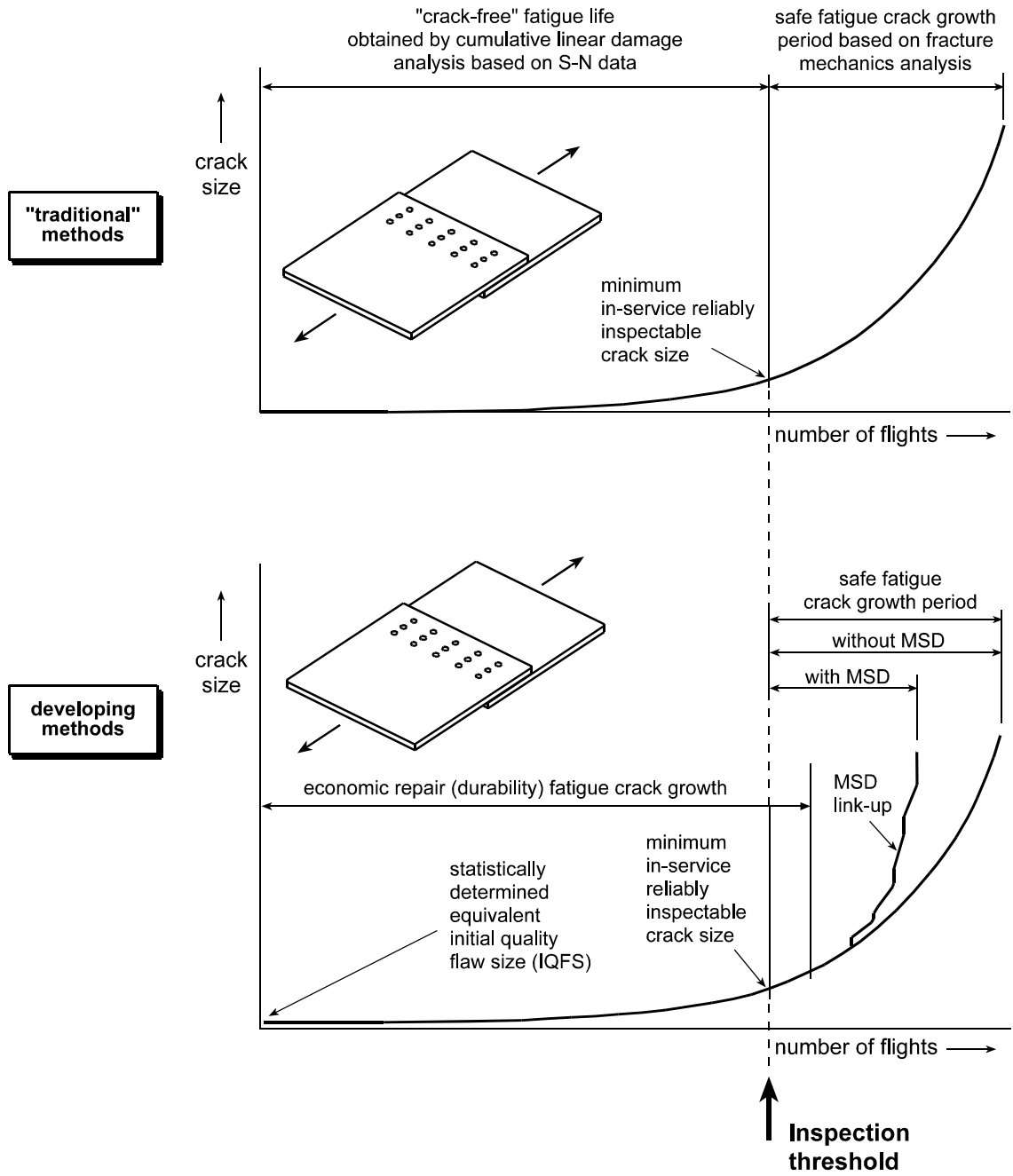


Fig. 22 Fatigue analyses for transport aircraft fuselage lap splices

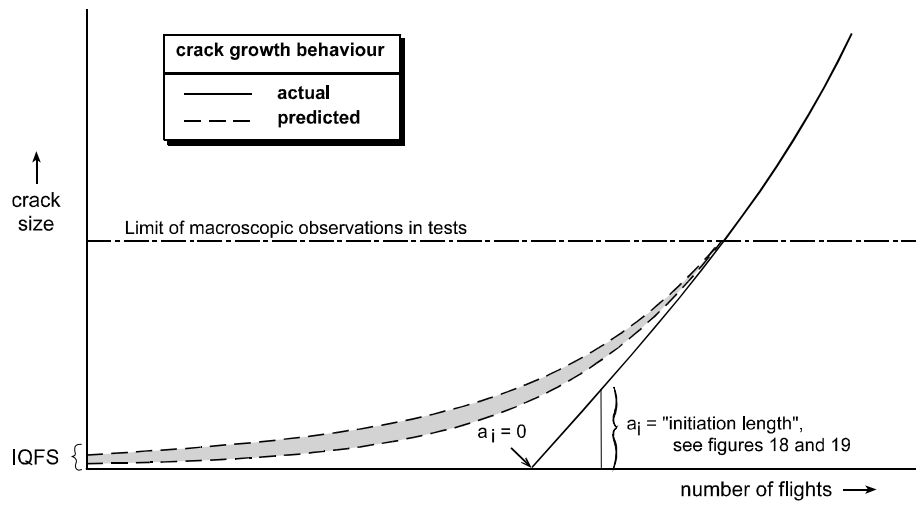


Fig. 23 Schematic of differences between actual and predicted early crack growth behaviour in transport aircraft fuselage longitudinal lap splices: the predictions are fitted to the macroscopic observations and the IQFS values are obtained from actual manufacturing flaws or by back-extrapolation using a macroscopic (long) crack growth model